

Accuracy Investigation for Structured-light Based Consumer 3D Sensors

JAN BOEHM, London

Keywords: Consumer, Gaming, Kinect, Repeatability, Accuracy

Summary: This work focuses on the performance investigation of consumer 3D sensors with respect to their repeatability and accuracy. It explores currently available sensors based on the 3D sensing technology developed by PrimeSense and introduced to the market in the form of the Microsoft Kinect. Accuracy and repeatability can be crucial criteria for the use of these sensors outside their intended use for home entertainment. The test strategies for the study are motivated by the VDI/VDE 2634 guideline. At the core of the work is the investigation of several units of the Asus Xtion Pro and the PrimeSense Developer Kit and a comparison of their performance. Altogether eighteen sensor units were tested. The results of the proposed test scenario for the sensor units show excellent repeatability at a few millimetres. However, absolute accuracy is worse and can be up to a few centimetres. Sensor performance varies greatly both for sensors of the same manufacturer and in-between manufacturers.

Zusammenfassung: *Genauigkeitsuntersuchung von Sensoren basierend auf strukturierter Beleuchtung aus der Unterhaltungselektronik.* Diese Arbeit zielt auf die Untersuchung der Leistungsfähigkeit von 3D Sensoren für Heimunterhaltung bezüglich ihrer Wiederhol- und Absolut-Genauigkeit. Es werden die momentan verfügbaren Sensoren untersucht, die auf dem Verfahren zur 3D Erfassung der Firma PrimeSense basieren und durch die Markteinführung der Microsoft Kinect populär wurden. Absolut- und Wiederhol-Genauigkeit können wichtige Faktoren sein, die über den Einsatz dieser Sensoren in Anwendungsfeldern außerhalb der Heimunterhaltung entscheiden. Die Teststrategien für die Untersuchung, die auf den Empfehlungen der VDI/VDE Richtlinie 2634 beruhen, werden vorgestellt und motiviert. Den Kern der Arbeit bilden die Tests und der Vergleich der Sensortypen Asus Xtion Pro und PrimeSense Developer Kit. Insgesamt wurden achtzehn Sensoren getestet. Die Untersuchungen zeigen eine gute Wiederholgenauigkeit von wenigen Millimetern. Die Absolut-Genauigkeit ist deutlich schlechter und kann bis zu mehrere Zentimeter betragen. Die Leistungsfähigkeit der Sensoren variiert stark sowohl für Sensoren desselben Herstellers als auch zwischen verschiedenen Herstellern.

1 Introduction

In recent years, we have seen increased development of consumer 3D sensors for home entertainment and video gaming. One motivation for the development of consumer 3D sensors is to lower the barrier in the interaction of man and machine by gesture recognition, also referred to as natural user interaction. Different sensor systems for capturing human gestures were proposed in the past and have been commercially explored. Many of these consumer 3D sensors can also be interesting for applications outside the home entertainment. 3DV System Ltd. developed a time-of-flight (TOF) range camera which captured human body poses and motions and was demonstrated in conjunction with a boxing game (YAHAV et al., 2007). 3DV System later sold its assets to Microsoft (SHELAH, 2009). Optrima NV also developed a time-of-flight range camera for natural user interaction (VAN NIEUWENHOVE, 2011) which is still available for developers. Optrima later merged with SoftKinetic who provide the software stack to detect human gestures. The current market leader PrimeSense developed a triangulation based range camera for natural user interaction. They also provide the software stack for gesture detection and skeleton extraction. PrimeSense have licenced their sensor technology to Microsoft and Asus. Recently PrimeSense Ltd. was acquired by Apple Inc. (WAKABAYASHI, 2013).

Whilst these sensors and the underlying technology have been available for several years, interest in them remained low. Interest grew with Microsoft's release of a motion sensing input device - the Microsoft Kinect - for their video game console Xbox 360. Within the first 10 days, Microsoft sold 1

million units of the sensor (MICROSOFT CORP., 2010). In the following 5 months, they sold altogether 10 million units. Compared to the sales figures of traditional three-dimensional sensors typically used in the photogrammetric community such as laser scanners and stripe projection systems these figures are enormous. The price of a Kinect in the meantime has fallen just below 100 EUR, which makes it one of the most affordable 3D sensors today.

While the Kinect originally was intended only for the use with Microsoft's video game console it soon gained interest in other application areas because of its affordability and versatility. Applications of the Kinect include tasks typical for 3D sensors such as 3D scene reconstruction (NEWCOMBE et al., 2011). They also include medical application such as the detection of patient's positions for radiation therapy (BAUER et al., 2011). Even rather surprising engineering tasks have been attempted with the Kinect such as the capturing of turbulent gas flows (BERGER et al., 2011). A large online community has gathered around the topic and is actively sharing knowledge on the devices. Part of that knowledge has recently been compiled in a book by KRAMER et al. (2012).

While for some application areas the affordability and relative simplicity of the system already are sufficient factors, other applications require performance criteria related to the accuracy of the obtained 3D coordinates. It is thus of obvious interest to investigate the performance of consumer 3D sensors intended for entertainment as generic 3D sensors. This work describes an approach to test consumer 3D sensors based on the PrimeSense technology. It summarizes the results obtained and concludes with some recommendations regarding their use.

2 Related Work

In the past accuracy investigations of generic 3D sensors delivering 3D data at video rate have mainly been performed for TOF cameras. Here the major issues are related to the stability of the frequency generator, scattering both internal to the instrument and in the scene and temperature related drifts (LICHTI & KIM, 2011; BOEHM & PATTINSON, 2010; KAREL, 2008; KAHLMANN ET AL., 2006). Test setups usually contain photogrammetric test fields using planar circular black and white targets. This is possible since most TOF cameras provide a perfectly registered intensity image as part of the acquisition principle. Section 4 gives a reason why this is not so simple in the case of fixed pattern projection used with the PrimeSense technology.

MENNA et al. (2011) have reported their approach for testing geometric accuracy of a Microsoft Kinect. They have also attempted a calibration using a photogrammetric camera model to improve the accuracy of the device. Other popular calibration methods for the Kinect include the software provided by BURRUS (2012).

Interference can be observed in-between sensors of the type discussed here and more detail is given in Section 4.1. MAIMONE & FUCHS (2012) suggest a hardware addition to the sensors to avoid this effect altogether. Using a small motor attached to each sensor the sensor is continuously shaken. This motion creates a blur on all externally projected patterns. This helps to disambiguate patterns. On the downside, the authors note an "increase in measurement instability".

This work follows the VDI/VDE guideline for acceptance test and verification of optical measuring systems 2634 part 2 (VDI, 2002). The guideline was established by a joint committee of the Association of German Engineers (VDI) and the German Society for Photogrammetry, Remote Sensing and Geoinformation (DGPF) (LUHMANN & WENDT, 2000). VDI/VDE 2634 is a "black-box" test that tries to abstract from particular sensor types or ranging principles. There is no attempt in this work to calibrate the sensor either. Rather the performance is tested "out of the box". This approach is complementary to the work of KHOSHELHAM & ELBERINK (2012), who attempt to establish and calibrate a mathematical sensor model. VDI/VDE 2634 uses known geometries (planes & spheres) and distances in-between known geometries to establish accuracy criteria. This differs from approaches where point clouds are compared directly to reference point clouds, e.g. using tools such as (CloudCompare, 2012). Previous tests have often only considered a single sensor. Since these sensors are mass-produced, it is important to test several units from different manufacturers. This allows observing the variation of sensor performance due to the mechanical packaging the manufacturer has chosen and observing variations among the same models due to manufacturing tolerances.

Field of View (Horizontal, Vertical, Diagonal)	58° H, 45° V, 70° D
Depth Image Size	VGA (640x480)
Operation range	0.8m - 3.5m
Spatial x/y resolution (@2m distance from sensor)	3mm
Maximal image throughput (frame rate)	60fps

Tab. 1: Specifications in the datasheet of the PrimeSensor reference design.

3 Sensor Technology

As mentioned above the work concentrates on the sensor technology developed by PrimeSense and licensed among others to Microsoft and Asus. Fig. 1 shows the family of sensors. PrimeSense describe their technology as light coding, which “works by coding the scene volume with near-IR light” (PrimeSense, 2011). More commonly the technology can be described as active triangulation or structured light using fixed pattern projection. The pattern is a speckle dot pattern generated using a diffractive optical element and a near-infrared laser diode. A close-up of the projected pattern is shown in Fig. 2 (left). PrimeSense has implemented the image processing as a system on a chip (SOC), which is offered as the PS1080. In addition, they offer a sensor reference design named the PrimeSensor.

The manufacturer provides a datasheet for the reference design, which is summarized in Tab. 1. There is no specific mention of accuracy in 3D space. Providing such information will be a key task in this work. Simple photogrammetric considerations allow us to estimate the theoretical limits of the accuracy in Z . The distance of the infrared projector and the infrared camera and thus the triangulation baseline is approximately 75 mm. At a distance of 1 m, the base to height ratio is smaller than 1:13. Photogrammetric rule of thumb recommends it should not fall much below this ratio (LUHMANN, 2000). This is the reason why the entire tests in the following sections are performed at a distance of 1 m. With the stated field of view, one can define a measurement volume for the tests of 1.1 m x 0.8 m x 0.5 m. The body diagonal of this volume L_0 is 1.45 m.

A theoretical derivation of the accuracy in depth measurement using the well-known triangulation formula is given by MENNA et al. (2011). The PS1080 considers the theoretical accuracies for the transfer of the data from the sensor to the host computer. In order to keep to the bandwidth limit of USB 2.0 the disparity images are transferred in compressed format. The compression effectively is a reduction to 11 bits. However, this is not an equidistant quantization in range, but in disparity. Therefore when converted to distance, the quantization steps vary. The quantization step width was experimentally determined across the depth range of the sensor. At 1 m depth, it is about 3 mm. This effect can be seen in Fig. 3, where the point cloud on a sphere is partitioned into layers of identical depth values. At 2 m, the quantization step already exceeds 10 mm and at 3 m, it exceeds 20 mm. These values perfectly match the theoretical values determined by MENNA et al. (2011). Therefore, one can argue that no accuracy is lost due to the compression. On the other hand, the quantization of depth values introduces step artefacts into the point cloud data, which make surface reconstruction difficult.

The pixel matrix of a single depth frame is only 640 by 480. This is small compared to colour cameras as available on the market today. However, it is larger than most competing TOF cameras. It is very interesting to compute the maximum point sampling rate from the number of points of a single frame and the maximum frame rate at VGA resolution, which is 30 frames per second. The 60 frames per second listed in the data sheet are valid for half-VGA resolution. This calculation gives us a point sampling rate of 9216000 points per second. This point rate outperforms current terrestrial laser scanning technology by an order of magnitude.

Sensors based on this reference design are available to developers from different manufacturers. Fig. 1 shows the currently available sensors. The left column image shows from top to bottom: the Microsoft Kinect, the PrimeSense Developer Kit (PSDK), the Asus Xtion Pro Live including a colour camera and the Asus Xtion Pro without the RGB camera. The images in the right hand column of Fig. 1 show the mechanical packaging for three of those sensors in the same order (Xtion Pro and Xtion Pro Live have the same packaging).

The Microsoft Kinect has additional features besides the 3D sensor, such as stereo microphones for user voice locating, a servo for tilting and a tilt sensor. Therefore, the footprint of this sensor is the largest. The optical components involved are the infrared projector, the colour camera and the infrared camera. They are mounted on what appears to be a pressed sheet metal strip. Additional circuit boards carrying the electronics are stacked on the back onto the same plate. From hands-on experience, it seems this unit is the least stable in the mechanical layout concerning the relative orientation of the optical components. This is obviously crucial for the repeatability of the 3D measurements. The PSDK has a much smaller footprint and a more stable closed metal frame. However, the optical components are mounted directly onto the circuit board. This again is not ideal for mechanical stability of the orientation of the individual components. The Asus Xtion Pro shown in the last image is slightly wider than the PSDK but more slender. The frame is an aluminium cast bracket. The optical elements are mounted directly onto the bracket using screws. The model shown here does not have a colour camera. The spot for the missing camera can be clearly seen next to the infrared camera with the four holes for the screws.

4 Repeatability

For testing the repeatability of the sensor, reference objects shall be measured repeatedly and any deviations shall be recorded. Typically, the objects are single signalized points. In photogrammetry, typically planar circular targets are used to signalize such points. The PrimeSensor is a triangulation device using an infrared camera and it is possible to access the images acquired by this infrared camera. Therefore, theoretically one could have followed the photogrammetric approach. However, the projected pattern disturbs intensity structures in the scene observed by the camera. Fig. 2 (left) shows

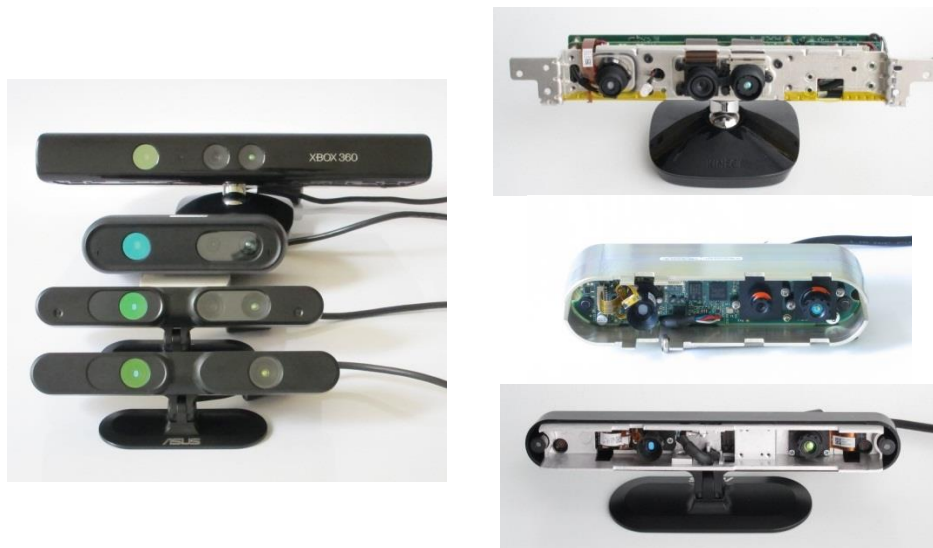


Fig. 1: Left image: Microsoft Kinect, PrimeSense PSDK, ASUS Xtion Pro Live and ASUS XTION Pro (top to bottom). The identical layout of the optical components (projector and cameras) is clearly visible. The right column shows the partially disassembled sensors: Microsoft Kinect, PSDK, ASUS Xtion Pro (top to bottom). The ASUS Xtion Pro is missing the colour camera. The Xtion Pro Live with colour camera is not shown disassembled, but has an identical layout to the Xtion Pro.

an example for a photogrammetric target under the projector illumination. It is very difficult to measure the centre of the target precisely with the disturbance from the pattern. Therefore, this work did not follow a photogrammetric approach but followed a generic 3D sensor approach and used spheres to signalize points in space. The centre is estimated from the points measured on the surface of the sphere via a best-fit sphere. Spheres with a diameter of 145 mm were chosen, which are typically used to register terrestrial laser scans (see Fig. 2 right). These spheres satisfy the criteria of the VDI/VDE 2634 guideline, which recommends a diameter of $(0.1 \dots 0.2) \cdot L_{\theta}$.

4.1 Interference between sensors

An additional issue interesting to test is potential interference between sensors. Since the devices use a static pattern projector, the projected dots will superimpose when two sensors share a common field of view. This can potentially cause a problem when the sensor's decoding algorithm tries to disambiguate the projected pattern. This effect is often referred to as interference between two sensors. This is clearly not interference in a physical or optical sense, where the superimposition of two wavelengths creates a new wavelength. The interference in-between sensors can occur in two ways.

For one the intensities of the two projected patterns add up. Therefore, locally the image of the infrared camera can become too bright and the imaging chip saturates locally. The 3D sensor is then unable to perform any measurement in these areas, which causes gaps in the point cloud. This occurs more frequently on surfaces of high reflectivity. It is possible to adapt the gain of the imaging chip to compensate for this. However, for scenes with surfaces of varying reflectivity and in situations of only partial overlap of two projected patterns it is not trivial to pick the correct gain.

The second form of interference occurs when the matching of the expected pattern and the acquired pattern fails due to the superimposition of two patterns in the scene. In this case, the disparities are estimated falsely. This leads to deviations in the depth values. The same effect could occur when the pattern emitted from the sensor itself is reflected on the scene twice due to scattering. For TOF cameras, this is a well-documented effect often referred to as scattering. This could happen in the proposed setup in Fig. 4 where the white wall might reflect the pattern back onto the spheres. However, no problems were encountered with such secondary projections. It seems the intensity of the scattered pattern is low enough not to disturb pattern identification.

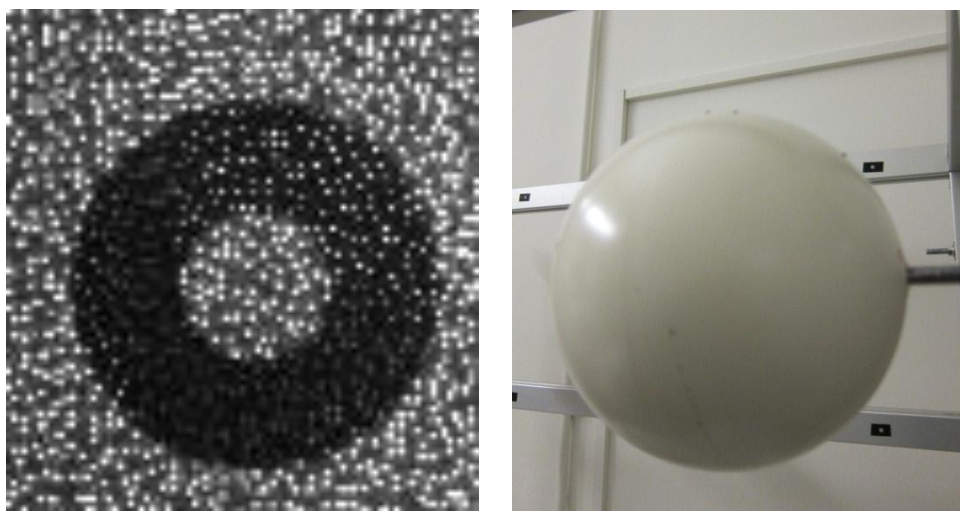


Fig. 2: Different target designs for marking reference points in the scene. A planar circular target (left) and a sphere (right). The fixed pattern projection makes precise measurement of photogrammetric targets difficult.

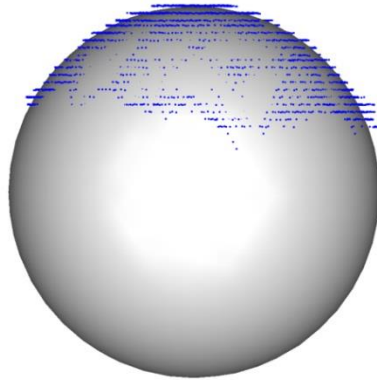


Fig. 3: Side shot of a pointcloud on the surface of a sphere of 145 mm diameter to show the quantization effect. The distance of the quantization „slices“ is 3 mm.



Fig. 4: Experiment set up for testing repeatability. The sensor under investigation is the leftmost sensor. Additional sensors are used to create pattern interference. Two spheres are used as targets.

The motivation for operating more than one sensor at the same time is typically to enlarge the measurement volume or avoid occluded areas. Therefore, two obvious geometric arrangements of two sensors were investigated: a parallel arrangement and an oblique arrangement. The parallel arrangement represents a scenario where the field of view is increased by placing sensors along a line with identical viewing direction, e.g. along a corridor. The oblique arrangement is representative for a circular arrangement, e.g. around an object with viewing directions towards the object's centre.

The setup for the experiments is shown in Fig. 4. Two spheres at a distance of 0.5 m from each other were observed by a single Asus Xtion Pro sensor mounted directly above the two spheres at a distance of 1 m. Two additional Asus Xtion Pro sensors were included in the setup to test interference of the pattern projection. A second sensor was added at 0.5 m distance to the sensor under investigation

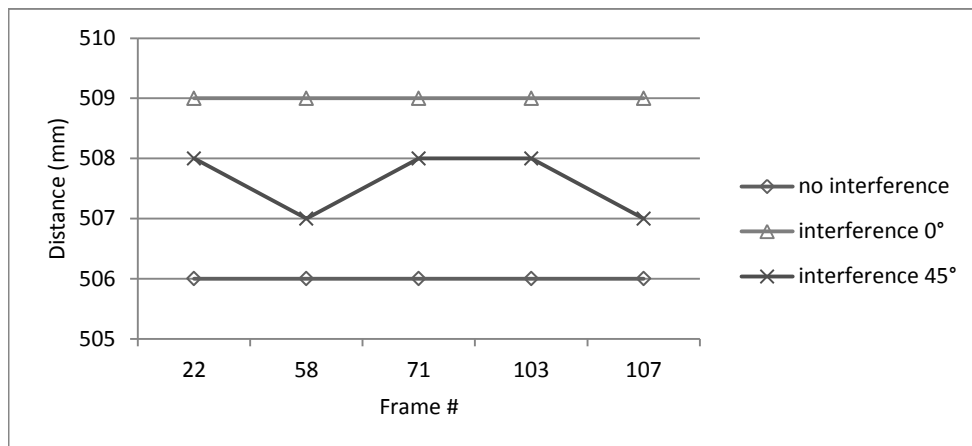


Fig. 5: Repeated measurement of the distance of two spheres with and without interference of the projected pattern.

and a viewing direction parallel to that of the first sensor (0 degree). A third sensor was mounted at a distance of 1 m at a viewing angle tilted 45 degrees with respect to the first sensor.

The results of the experiment are summarized in Fig. 5. It shows the distance measurements of five frames out of a sequence of frames acquired with the constant setup. Single frames were used for the evaluation and no averaging over frames was done. When only one sensor was activated, the distance of the two spheres was measured at exactly the same value to the mm. These are extremely encouraging results as far as repeatability is concerned. When interference was generated from a 0 degree angle the distance measurement was offset by 3 mm, but again remained constant. When interference was generated from a 45 degree angle the distance measurement varied slightly at an offset of 1-2 mm. Considering that the expected measurement accuracy at this distance is only 3 mm these variations are rather small. While some degree of interference between sensors did occur, the alterations to the measurements seem to be small. Interference between sensors is therefore not considered for the following experiments on absolute accuracy.

5 Accuracy

5.1 Flatness and Probing

The VDI/VDE guideline for acceptance test and verification of optical measuring systems 2634 part 2 (VDI, 2002) is a good recommendation for a generic test of a 3D sensor based on area scanning. The experiments adhere to this guideline where possible. VDI/VDE 2634 defines the quality parameter *flatness measurement error* R_E as “the range of the signed distances of the measuring points from the best fit plane”. Fig. 6 (left) shows the result of a single measurement of a plane from an Asus Xtion Pro. In contradiction to the requirements of the guideline, there is no calibration certificate for the plane, but with respect to the expected accuracy of the measurements, flatness was sufficient. The standard deviation of the points to the fitted plane is 2.7 mm. However, the maximum deviation is ± 19 mm. So according to the guidelines the flatness measurement error R_E is 38 mm. The maximum deviations occur at the very corners of the field of view, where the point cloud sharply either bends away from or towards the sensor.

Another quality parameter defined in VDI/VDE 2634 is the *probing error* R , which describes the characteristics of the sensor within a small part of the measurement volume (10-20% of L_0). It is defined as “the range of the radial distance between the measured points and a best-fit sphere.” Fig. 6 (right) shows deviations on a sphere of 145 mm diameter. The standard deviation is 1.3 mm and the maximum deviation is ± 6 mm. This gives a probing error R of 12 mm. These tests show that the point cloud data delivered from the PrimeSensor generally follows the 3D shape of the object – indicated by good standard deviations. However, there are clearly outliers in the measured point cloud.

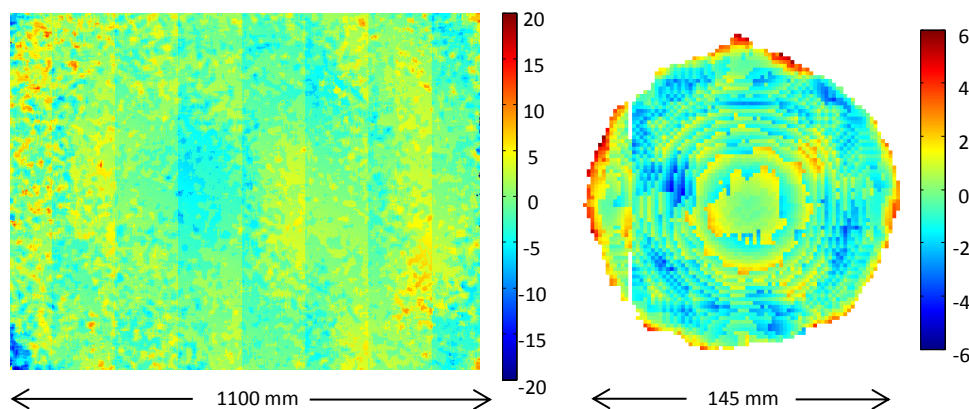


Fig. 6: Test results for flatness measurement error and sphere fit (probing error). Both measurements are taken at 1 m distance. The colour scale is in mm.

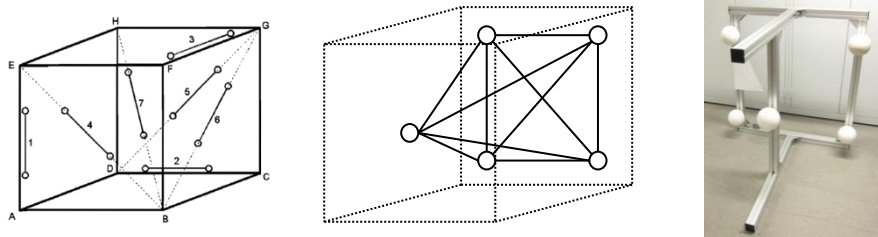


Fig. 7: VDI/VDE 2634 recommendations for the arrangement of the reference distances in the measurement volume (left). Arrangement of 10 reference distances used in this work (centre). Actual structure with spheres used for experiments (right).

5.2 Sphere Spacing Error

While flatness and probing indicate the ability of a sensor to capture the shape of an object they do not assess a sensor's ability to accurately keep measurements to scale across the measurement volume. VDI/VDE 2634 therefore defines the quality parameter *sphere-spacing error* (*SD*) to verify the capability to measure lengths. The sphere spacing error Δl is defined as "the difference between the measured and calibrated values of the distance between the centres of two spheres". The guideline recommends taking the measurement of 7 different distances of two spheres in the volume. The permissible limit for these measurements is *SD*. Fig. 7 (left) shows the recommended arrangement of the 7 distances in a measurement volume. A pyramidal structure is used containing 5 spheres to represent 10 distances in a volume of 1.1 m x 0.8 m x 0.5 m. Fig. 7 (middle) shows the orientations of the 10 distances. Fig. 7 (right) shows the actual frame that was used for the experiments. A Faro Photon 120 laser scanner (FARO, 2009) was used to establish reference values for the distances between the spheres. The 3D sensors were placed on a tripod at 1 m distance from the frame centre facing the tip of the pyramid. A quick release plate for the tripod head was used with the PSDK to insure repeatable positioning. For the ASUS Xtion Pro a mechanical block was used to enable re-positioning of swapped sensors.

Fig. 8 shows the deviations of the measurements from a single Asus Xtion Pro to the reference values over the lengths, where the length vary from 0.7 to 1.2 m. The deviations range from a maximum (positive) deviation of +2 mm to a minimum (negative) deviation of -9 mm. In this case, the span is 11 mm and *SD* could be set to this or any larger value.

This experiment was repeated for 10 different units of the Asus Xtion Pro. For each sensor, the maximum (positive) and minimum (negative) deviation were recorded. Fig. 9 summarizes the results. All sensors clearly keep within a band of +10 mm to -20 mm. However, there are large differences between the sensors. Some sensors have only a small span between maximum and minimum deviation, which is well distributed around zero, for example 5 mm for sensor #10. Other sensors exhibit a large span of up to 20 mm. For some sensors the negative deviations clearly dominate.

In order to compare sensors based on the PS1080 from different manufacturers, the measurements were repeated for 8 units of the PrimeSense PSDK in addition to the 10 ASUS units. Fig. 10 shows the results from the Asus Xtion Pro and the results of the PSDK in one graph. It is apparent that the PSDK typically has a much larger span between maximum and minimum deviation than the Xtion Pro. There are cases of deviations of almost 100 mm. On average, the span for the PSDK is 40 - 50 mm. One might attribute this drop in performance to the less stable mechanical packaging of the optical components of the sensor, which is described in Section 3. A lack in stability might lead to an invalidation of the initial factory calibration of the device over time.

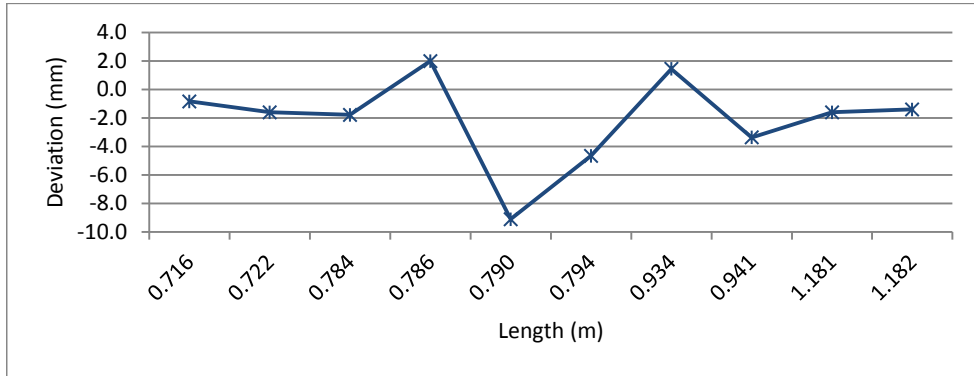


Fig. 8: Deviations in the sphere spacing measurements of a single Asus Xtion Pro unit.

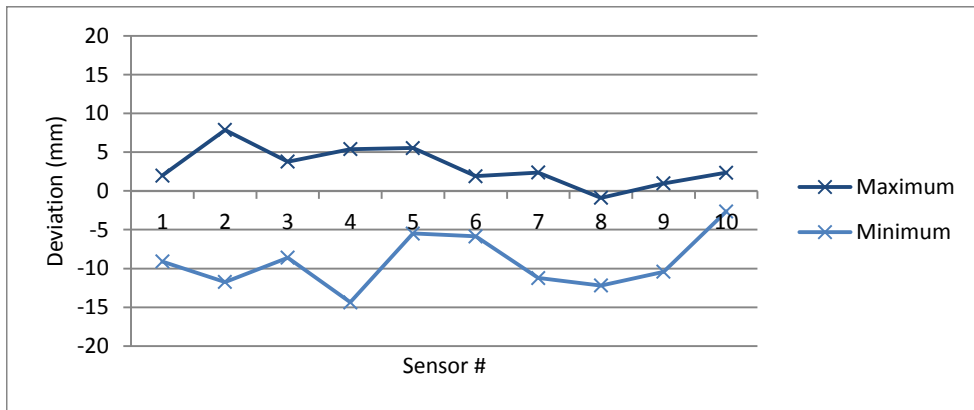


Fig. 9: Minimum and maximum sphere spacing deviations of ten different Asus Xtion Pro units.

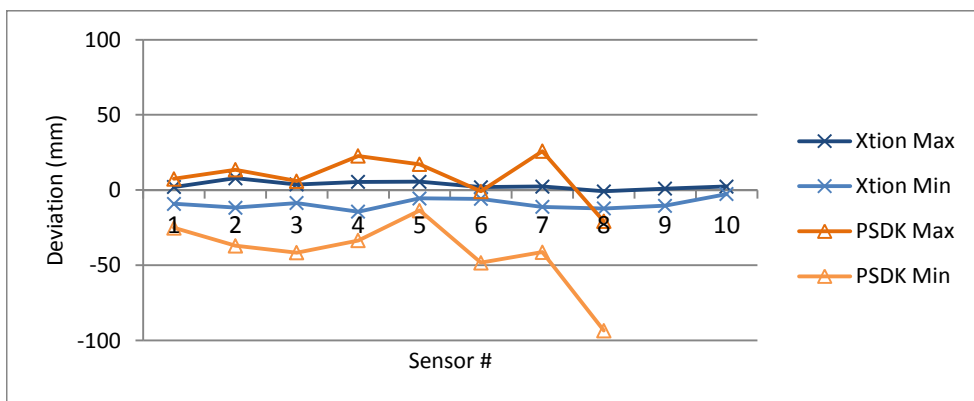


Fig. 10: Comparing maximum and minimum sphere spacing deviations of ten Asus Xtion Pro units to eight PrimeSense PSDK units.

6 Conclusions

This article has demonstrated the performance of a group of consumer 3D sensors based on the PrimeSensor reference design. The sensors can be used as generic 3D sensors or range cameras beyond their intended use for entertainment. However, some caution ought to be observed when using these sensors for specific applications. Due to the small baseline, the performance degrades rapidly at larger depth (MENNA ET AL., 2011). An appropriate measuring volume has to be chosen carefully. This issue is deepened by the quantization of depth values. While the data delivered from the sensors follows the general shape of a 3D scene quite well, there are considerable outliers in the data. While repeatability of the measurements is quite good, the absolute accuracy is less impressive. Different units of the same sensor type vary quite strongly. The same can be said about the performance of sensors of similar design from different manufacturers. For some applications, it might be recommended to select the units, i.e. test the performance of a larger set of sensors and only put the better ones to use. Considering the low cost of a single unit, this will still give an impressive price-performance ratio. Looking at the different mechanical packages offered for the PrimeSensor, it seems advisable to look for mechanical stability, in order to achieve good measurement results.

Acknowledgement

The author would like to thank the anonymous reviewers for their valuable comments and suggestions to improve the quality of the paper.

References

- BAUER, S.; WASZA, J.; HAASE, S.; MAROSI, N.; HORNEGGER, J., 2011: Multi-modal surface registration for markerless initial patient setup in radiation therapy using microsoft's Kinect sensor. – Computer Vision Workshops (ICCV Workshops), pp. 1175 – 1181.
- BERGER, K.; RUHL, K.; ALBERS, M.; SCHRODER, Y.; SCHOLZ, A.; KOKEMULLER, J.; GUTHE, S.; MAGNOR, M., 2011: The capturing of turbulent gas flows using multiple Kinects. – IEEE Computer Vision Workshops (ICCV Workshops), pp. 1108 – 1113.
- BOEHM, J., PATTINSON, T., 2010: Accuracy of exterior orientation for a range camera. – The International Archives of the Photogrammetry, Remote Sensing and Spatial Information Sciences 38 (Part 5), pp. 103 – 108.
- BURRUS, N., 2012: Kinect Calibration. – <http://nicolas.burrus.name/index.php/Research/KinectCalibration>
- CLOUDCOMPARE [GPL software], 2011. EDF R&D, Telecom ParisTech. Retrieved from <http://www.danielgm.net/cc/>.
- FARO, 2009. FARO Laser Scanner Photon 120/20. - www.faro.com/adobe_pdf_mgr.aspx?item=969&pdfTitle=FARO_Photon_en_pdf
- KAHLMANN, T., REMONDINO, F., INGENSAND, H., 2006: Calibration for increased accuracy of the range imaging camera SwissRanger. – International Archives of Photogrammetry, Remote Sensing and Spatial Information Sciences, Vol. XXXVI, part 5, pp. 136-141.
- KAREL, W., 2008: Integrated range camera calibration using image sequences from hand-held operation. – The International Archives of Photogrammetry, Remote Sensing and Spatial Information Sciences, Vol. XXXVII, part 5, pp. 945-951.
- KHOSHELHAM, K., ELBERINK, S. O., 2012: Accuracy and Resolution of Kinect Depth Data for Indoor Mapping Applications. – Sensors, 12, 1437-1454.
- KRAMER, J., BURRUS, N., HERRERA, C.D., ECHTLER, F., PARKER, M., 2012: Hacking the Kinect – Apress.

- LICHTI, D.D., KIM, C., 2011: A comparison of three geometric self-calibration methods for range cameras. – *Remote Sensing*, 3 (5), pp. 1014-1028.
- LUHMANN, T., 2000: Nahbereichsphotogrammetrie. – Wichmann.
- LUHMANN T., WENDT K., 2000: Recommendations for an acceptance and verification test of optical 3-D measurement systems. – *International Archives of Photogrammetry, Remote Sensing and Spatial Information Sciences*, Vol. XXXIII, part 5, pp. 493–499.
- MAIMONE, A., FUCHS, H., 2012: Reducing Interference Between Multiple Structured Light Depth Sensors Using Motion. – *IEEE Virtual Reality Workshops (VR)*, pp. 51 – 54.
- MENNA, F., REMONDINO, F., BATTISTI, R. AND NOCERINO, E., 2011: Geometric investigation of a gaming active device. – *Proc. SPIE 8085*, 80850G.
- MICROSOFT CORP., 2010: Kinect for Xbox 360 Hits Million Mark in Just 10 Days. – Press Release, Redmond, Washington Nov. 15
- NEWCOMBE, R.A., IZADI, S., HILLIGES, O., MOLYNEAUX, D., KIM, D., DAVISON, A.J., KOHLI, P., SHOTTON, J., HODGES, S. AND FITZGIBBON, A., 2011: KinectFusion: Real-Time Dense Surface Mapping and Tracking. – *ISMAR '11 Proceedings of the 2011 10th IEEE International Symposium on Mixed and Augmented Reality*, pp. 127 – 136.
- VAN NIEUWENHOVE, D., 2011: Optrima Technology Overview about DepthSense and OptriCam. – *International Workshop on Range-Imaging Sensors and Applications (RISA)*, January 27-28, 2011, Trento, Italy.
- PRIMESENSE, 2011: PrimeSensor Datasheet. – <http://www.primesense.com>.
- SHELAH, S., 2009: Microsoft confirms 3DV acquisition. – *Globes [online]*, Israel business news - <http://www.globes.co.il/serveen/globes/docview.asp?did=1000460733>
- VDI, 2002. VDI/VDE 2634 Part 2 - Optical 3D measuring systems – Optical systems based on area scanning.
- WAKABAYASHI, D., 2013: Apple Acquires Israel's PrimeSense. – *The Wall Street Journal Blog* - <http://blogs.wsj.com/digits/2013/11/25/apple-acquires-israels-primesense/>
- YAHAV, G., JDDAN, G.J., MANDELBOUM, D., 2007: Camera for Gaming Application using a novel 3D Imager. – *8th Conference on Optical 3-D Measurement Techniques*, July 9-12, 2007, ETH Zurich, Switzerland.

Address of the Author:

Dr.-Ing. JAN BOEHM, University College London, Department of Civil, Environmental and Geomatic Engineering, Gower Street, London, WC1E 6BT UK, Tel.: +44-20-3108-1036, e-mail: j.boehm@ucl.ac.uk